Title	Processes affecting long-term changes in ^{137}Cs concentration in surface sediments off Fukushima
Author(s)	Otosaka Shigeyoshi
Citation	Journal of Oceanography, 73(5), p.559-570 (2017).
Text Version	Author Accepted Manuscript
URL	https://jopss.jaea.go.jp/search/servlet/search?5057599
DOI	https://doi.org/10.1007/s10872-017-0421-5
Right	This is a post-peer-review, pre-copyedit version of an article published in Journal of Oceanography. The final authenticated version is available online at: https://doi.org/10.1007/s10872-017-0421-5

Processes affecting long-term changes in ^{137}Cs concentration in surface sediments off Fukushima

Shigeyoshi Otosaka

Research Group for Environmental Science, Japan Atomic Energy Agency, 2-4 Shirakata, Tokai, Ibaraki 319-1195, Japan

Phone +81.282.5171, FAX +81.282.6760

Email otosaka.shigeyoshi@jaea.go.jp

Abstract

Temporal changes in cesium-137 (^{137}Cs) concentrations in the surface (0-10 cm) layer of seabed sediment were quantified from continuous observation data at 71 stations within a 150 km radius of the Fukushima Daiichi Nuclear Power Plant, and the primary processes affecting temporal changes were identified. From March 2011 to the end of 2015, about 80% of the initially-deposited ^{137}Cs in the surface sediment in the coastal region (bottom depth ≤100m) region has dissipated (radioactive decay is not included). Such a remarkable change in the ^{137}Cs concentration was not observed in the offshore (>100m) region. This paper focuses on the following three processes that affected the decrease in the ^{137}Cs concentrations, and assesses their relative importance; (1) resuspension and transport of ^{137}Cs-bound sediment, (2) desorption of ^{137}Cs from the sediment, and (3) dilution of ^{137}Cs by vertical mixing of sediment. Consequently, it was estimated that the first two processes together have potentially contributed to reduce the ^{137}Cs inventory in the top 10 cm of the coastal region by at most 35%. Furthermore, by applying a pulse input sediment mixing model to the observed vertical distribution of sedimentary ^{137}Cs, it was also estimated that more than 43% of the ^{137}Cs in the surface sediment was transported to deeper sediment layers by vertical mixing of the sediment. This indicates that the decrease of ^{137}Cs concentrations in coastal sediments was mainly affected by mixing of ^{137}Cs-bound surface sediment with less-contaminated sediment in the deeper layers.

Keywords: Fukushima Daiichi Nuclear Power Plant accident, radiocesium, sediment, suspended particles, bioturbation, particle-seawater interaction

1. Introduction

Among the radionuclides released by the accident of Fukushima Daiichi Nuclear Power Plant (FDNPP), cesium-137 (^{137}Cs; half-life = 30.2 years) is a key radionuclide that should be monitored from a viewpoint of middle-term (~50 years) dose assessment (e.g., Saito et al., 2015). Within a year after the accident that occurred on March 11, 2011, 15-18 PBq of ^{137}Cs was released to the North Pacific (Buesseler et al., 2017), and about 1-2% of the ^{137}Cs in the ocean (0.2±0.05 PBq) was deposited onto the seabed (Otosaka and Kato, 2014).

Continuous monitoring showed that the concentration of ^{137}Cs in the surface seawater in the western North Pacific decreased over several orders of magnitude from 2011 to 2015, and has approached to the pre-accident level except for the vicinity of the FDNPP (e.g., NRA, 2016). The ^{137}Cs concentration in seabed sediment has also shown a decreasing trend, but the rate is slow relative to that in the seawater. Consequently, the general characteristics of the lateral distribution of ^{137}Cs in seabed sediment have remained over a long period.

The ^{137}Cs activity in fishes caught in the coastal area off Fukushima has decreased to an insignificant level for radiation dose (Okamura et al., 2016). A small portion of the radiocesium in the seabed, however, is in bioavailable fractions of the sediment (Ono et al., 2015; Otosaka and Kobayashi, 2013) and may be incorporated into the marine ecosystem through the benthic food web.

Iwata et al. (2013) reported that the ecological half-life of ^{137}Cs in common demersal fish (e.g., marbled sole) is 280-380 days, a few times longer than the biological half-life obtained from a controlled laboratory experiment. Estimations using a dynamic food chain transfer model pointed out that the concentration of ^{137}Cs in demersal fishes in the Fukushima coastal area cannot be explained only by the supply of ^{137}Cs via the surface seawater (Tateda et al., 2013), and there is another source supplying ^{137}Cs in the coastal environment (Tateda et al., 2017).

Thus, the importance of a clear understanding of the processes affecting the long-term change in the radiocesium concentration in the seabed sediments is needed in order to reconstruct the impact of the accident on the marine ecosystem, as well as to predict the effect of nuclear incidents which may take place in future.

In the region off Fukushima, Cs bound to seabed sediment is often resuspended and transported laterally according to the turbulent flow of the

bottom water current (Yagi et al., 2015; Otosaka and Kobayashi, 2013). Depending on the hydrographic conditions, such suspended particles sometimes are transported offshore where they are re-incorporated into the seabed (Ikehara et al., 2014; Buesseler et al., 2015).

It is known that the majority of radiocesium in sediments is tightly adsorbed on the surface of clay minerals and the mobility is relatively low. However, as mentioned above, desorbable ^{137}Cs is also found in seabed sediment (Otosaka and Kobayashi, 2013), suspended particles (Takata et al., 2015), and soils (Murota et al., 2016). Although the expected desorption rate is quite slow, such desorbable ^{137}Cs from the seabed sediment can be incorporated by the benthos (Wang et al., 2016).

Bioturbation and bioirrigation are key processes for the vertical mixing of the sediment particles and pore water (e.g. Teal et al., 2008). Such processes were observed in the coastal region of this study, even though the benthic ecosystems of this area were once severely affected by a tsunami in 2011 (Seike et al., 2016). Black and Buesseler (2014) suggested that bioturbation efficiently transports ^{137}Cs from the surface to deeper layers of the sediment. Additionally, in the shallower (~20 m) regions, wave-derived mixing of surface sediment occurs regularly (e.g., Sawaragi, 1995). Such vertical mixing of sediment also reduces the apparent ^{137}Cs concentrations in the surface sediment.

In this study, continuous monitoring data of seabed sediment in the surrounding region of Fukushima (~150 km radius from the FDNPP) were systematically compiled, to provide a more comprehensive understanding of the temporal changes in the inventory of sedimentary ^{137}Cs in the first 5 years after the accident. Furthermore, this study assessed the effects of the following major processes on the temporal change in the ^{137}Cs abundance: (1) resuspension and lateral transport of radiocesium-bound particles, (2) leaching of radiocesium from sediments, and (3) downward transport of sedimentary radiocesium due to vertical mixing of the sediment.

2 Methods

2.1 Data sources

Data from monitoring of ^{137}Cs in seabed sediment observed between 2011 and 2015 were used for the analysis. All data were obtained from the region within a 150 km radius of FDNPP. In addition to sediment data from 18 stations obtained by this study, data at 53 stations from monitoring programs of the Ministry of the Environment, Japan (MOE, 2013; 2016a; 2016b), and of the Tokyo Electric Power Co. (TEPCO), reported by the Nuclear Regulation Authority, Japan (NRA, 2016) were compiled in the dataset (Table 1, Fig. 1). For all stations, ^{137}Cs concentrations are from the top 10 cm of the sediment. The 0-10 cm layer was selected because it includes the sediment-water interface and important habitats for benthic biota that may affect the concentration of radionuclides in the ecosystem over decades. Topographic data for the TEPCO stations were obtained from the 1-minute Gridded Global Relief Data (ETOPO2v2) (NOAA, 2006).

2.2 Sampling and sample analysis

Seabed sediment was collected using a multiple corer or a Smith-McIntyre grab sampler. The sampling was carried out with cooperation of R/V Hakuho maru, R/V Tansei maru, R/V Daisan Kaiyo maru, R/V Shinsei maru, and the R/V Seikai. After recovery, core samples were cut into 1-2 cm intervals and kept in a freezer until further processing for analysis. After being transferred to a laboratory on land, sediment samples were dried at 105°C, the coarse fractions were removed using a 2-mm sieve, and crushed (IAEA, 2003). Polystyrene container (43 or 87 mL) were filled with the powdered samples, and specific gamma-rays of ^{137}Cs (661 keV) were measured using a coaxial Ge detector (ORTEC GEM20P4, 1.7 keV/1.33 MeV resolution and 29-31% relative efficiencies). Specific gamma-rays of ^{210}Pb (46.5 keV) and ^{214}Pb (352 keV) were measured using a low-energy photon detector (ORTEC LOAx-51370/20P, 0.625 keV/122 keV of resolution), and activities of the excess-^{210}Pb ($^{210}Pb_{ex}$) were calculated by subtracting ^{214}Pb activities from the ^{210}Pb activities on the assumption that the activities of the ^{226}Ra-derived ^{210}Pb is equal to those of ^{214}Pb. Concentrations of radiocesium

reported in the following sections are represented as Bq kg^{-1} dry weight. Activities of radiocesium were decay-corrected to March 11, 2011, and activities of $^{210}Pb_{ex}$ were decay-corrected to the date of sampling.

Water content and dry bulk density were measured with a given volume of plastic tube. From the measured ^{137}Cs activity and dry bulk density in each sample, cumulative ^{137}Cs concentration in the 0-10 cm sedimentary layer was calculated.

The loss upon ignition method was used to determine the organic matter content. Samples were heated in a muffle furnace at 500°C for 24 hours. Grain-size distributions of the defrosted (undried) sediment were measured using a laser diffraction particle size analyzer (Shimadzu, SALD-2000J). 0.1% pyrophosphoric acid solution was used as dispersant for the grain-size measurement.

2.3 Data analysis

2.3.1 Estimation of variation rates in ^{137}Cs concentrations in surface sediment

At most coastal stations, the decay-corrected ^{137}Cs concentrations in the sediment changed exponentially with time (see subsection 3.1). As a first step to assess the effect of factors affecting the temporal change, except for radioactive decay, the trend, for convenience, was expressed as an exponential curve (eq. (1)), and the exponent α was calculated,

$$I = I_0 \exp(\alpha \times \Delta t) \qquad (1)$$

where, I is ^{137}Cs concentration in the sediment, I_0 is ^{137}Cs concentration on the reference date (March 11, 2011), Δt is the elapsed time between the reference date and date of observations. Both ^{137}Cs activities of I and I_0 are decay-corrected to the reference date.

Based on the exponent α, the variation rate of ^{137}Cs activity in the seabed sediment (X) was calculated by eq. (2).

$$\boldsymbol{X}\ (\%) = (e^{\alpha} - 1) \times 100 \qquad (2)$$

Uncertainty of the variation rate at each station (u) was defined as eq. (3),

$$u = \sqrt{\frac{\sigma^2}{\sum(t_i - \bar{t})^2}} \qquad (3)$$

where, σ is variance of the average of ln [I] in each station, t_i is the i th data of time (t), and $\bar{t}$ is the average of t.

2.3.2 Evaluation of vertical mixing of surface sediment

The effect of vertical mixing of the sediment on the vertical distribution of ^{137}Cs was evaluated at 10 stations. A theoretical vertical distribution of ^{137}Cs at the date of observation was estimated using a 1-D biodiffusion model (Cochran et al., 1985), and then the effect of bioturbation was assessed by comparing the theoretical and observed vertical profiles of ^{137}Cs in the sediment.

In this biodiffusion model, a certain amount of ^{137}Cs (assumed to be the same as I, here) was set for the surficial sediment (0-1 cm layer), and "diffused" to the deeper layers with a biodiffusion coefficient D_b (eq. (4)).

$$C = C_0 \, exp \left(\frac{-z^2}{4D_b \Delta t}\right) \qquad (4)$$

where, C: ^{137}Cs activity, and Δt: time after the reference date (April 6, 2011) when the highest ^{137}Cs concentration was observed in the surface seawater of the coastal area of Fukushima (Oikawa et al., 2013).

At eight stations where a vertical gradient of $^{210}Pb_{ex}$ was observed, D_b values were calculated using eq (5).

$$A = A_0 \, exp \left(-\sqrt{\frac{\lambda}{D_b}} \, z\right) \qquad (5)$$

where, A: $^{210}Pb_{ex}$ activity, z: sediment depth, and λ: decay constant of ^{210}Pb (0.0312 year^{-1}). The eq (5) is based on the assumption that sedimentation is much smaller than bioturbation.

In the coastal stations where the gradation of $^{210}Pb_{ex}$ did not appear, a maximum D_b value was estimated assuming that the observed decreasing trend of ^{137}Cs concentration was controlled by the vertical mixing of sediment. The validity of the maximum D_b is discussed in subsection 4.3.

3. Results

3.1 Temporal change in ^{137}Cs concentration in the upper (0-10cm) sediment

The temporal change in ^{137}Cs concentrations in surface (0-10cm) sediment collected from the coastal area (bottom depth ≤100 m) of Miyagi, Fukushima, Ibaraki prefectures, and offshore (>100 m) are shown in Figs. 2a, b, c, and d, respectively. Except for the offshore stations (Fig. 2d), ^{137}Cs concentrations in the surface sediment generally showed a decreasing trend. Considering that the ^{137}Cs concentrations were decay-corrected to a reference date, these trends are not affected by radioactive decay, but by other processes leading to a decrease in radiocesium concentration in the seabed sediment.

As shown in Figs. 2b and 2c, the rate of decrease in ^{137}Cs in surface sediments seems to have slowed down with time. This may indicate that fitting of an exponential curve on this temporal change is not appropriate, but this study attempted to generalize trends systematically, and approximated the trends as exponential functions. Calculated exponents in Miyagi, Fukushima, and Ibaraki coastal areas were -0.0009±0.0004 day^{-1} (n = 32), -0.0009±0.0006 day^{-1} (n = 1,938), -0.0008±0.0002 day^{-1} (n = 58) respectively, and there was no clear regional difference in the exponents.

The exponents similarly calculated for surface seawater near the FDNPP were -0.05- -0.01 day^{-1} between 2011 and 2012 (Oikawa et al., 2013; Kanda, 2013), and about -0.001 day^{-1} between 2012 and 2015 (Buesseler et al., 2017). The exponents for demersal fishes caught in the coastal region were -0.001 - -0.002 day^{-1}, based on monitoring data (MAFF, 2016). The decrease of ^{137}Cs concentrations in coastal sediments was slower than that for seawater and similar to those in demersal fishes.

In the offshore region, no notable temporal change in ^{137}Cs concentrations was observed in the surface sediment (Fig. 2d) and values remained in the range of ca. 10 – 100 Bq kg^{-1}.

Relative variances between 2011 and 2015 calculated for four sediment parameters (dry bulk density, median diameter, organic matter content, and ^{137}Cs concentration) are listed in Table 2. In the calculation of the values in the table, relative standard deviations (RSD) were obtained for each station, then median and range of the RSDs were calculated for each parameter. Among the four parameters, dry bulk density showed the lowest variance, and the RSD calculated for 18 stations was less than 12% (median: 6.7%). The median RSDs of particle size and organic matter content were 15% and 29%, respectively. Median RSD of ^{137}Cs concentration was 43% (range: 1-124%), and was highest of the four parameters.

This result indicates that temporal change in the dry bulk density in the surface sediments of this study area is quite small, even though the ^{137}Cs concentration changed continuously between 2011 and 2015. Accordingly, we can consider that the temporal changes in ^{137}Cs concentration correspond to that of the ^{137}Cs inventory in the surface sediments.

3.2 Variation rate of ^{137}Cs inventory in surface sediment

In Figure 3, variation rates of ^{137}Cs in the surface sediment are plotted against bottom depth. The calculated variation rate ranged between -63% $year^{-1}$ and +54% $year^{-1}$, and were generally lower in the coastal (≤100 m depth) sediment, consists of medium and coarse sand. The geometric mean of the variation rate in the coastal region was -27% $year^{-1}$ (Table 3). This result suggested that the ^{137}Cs was dissipated from the surface sediment in the coastal region.

The variation rates in the offshore region (>100 m) plotted around 0% $year^{-1}$ except for a high rate (+48% $year^{-1}$) in Sta. FS1 where the smallest initial ^{137}Cs inventory was recorded (0.1 kBq m^{-2}, Appendix A2). The geometric mean of the variation rate in the offshore was +5% $year^{-1}$, and this result indicates that the inventory of sedimentary ^{137}Cs in the offshore region has remained relatively constant until the end of 2015.

In order to investigate the distribution of variation rates in the coastal region in detail, latitudinal distributions of the variation rate obtained from the 63 coastal stations (≤100 m: Fig. 4a) is shown in Figure 4b. The majority of the variation rates in Figure 4 ranged between -50- -10% year^{-1}. For the coastal stations, there was no notable latitudinal trend in the initial (2011) ^{137}Cs concentration in the surface sediment (Fig. 4c). Considering that the initial distribution of sedimentary ^{137}Cs concentration was established by contact of contaminated seawater with the sediment surface (Otosaka et al., 2014; Misumi et al., 2014), the latitude-independent distribution of sedimentary ^{137}Cs in Figure 4c would correspond the distribution of contaminated seawater in the initial stages after the accident. Consequently, the net change in the sedimentary ^{137}Cs (expressed as the "variation index": product of ^{137}Cs variation rate by concentration) differed markedly between some stations (Fig. 4d).

Incidentally, in Figure 4b, some coastal stations showed exceptionally high (> -10% year^{-1}) variation rates. These stations can be categorized into 3 groups; (i) 1 station, 145 km northeast of the FDNPP, (ii) 4 stations in the area 73-114 km south of the FDNPP, and (iii) 10 stations in the vicinity of the FDNPP. All stations in groups (i) and (ii) are located around the boundary between the coastal and offshore regions (71-95 m depth) and are far from the FDNPP. Therefore, we can consider that results from the groups (i) and (ii) showed features closer to those of offshore regions, rather than the coastal region.

Water depth of stations in group (iii), on the contrary, ranged between 5 m and 66 m (19 m in average). It is known that ^{137}Cs concentration in seawater of the FDNPP's harbor still has remained at more than 100 times higher than concentrations outside the harbor, although the level is decreasing with time (TEPCO, 2016). Considering that the harbor water exchanges with outside water at a certain rate (e.g., 44% day^{-1}: Kanda, 2013), the high variation rate observed in the group (iii) stations may be affected by continuing supply of local input of ^{137}Cs from the harbor or the neighboring regions. In fact, relatively high concentrations of ^{137}Cs are detected in surface seawater within 10 km radius of the NPP (Fukuda et al., 2016). Nevertheless, such areas showing "exceptionally" high variation rates are limited compared to the entire area investigated by this study.

3.3 Vertical profiles of ^{137}Cs in sediment

Vertical profiles of ^{137}Cs concentrations at 10 stations observed between 2012 and 2015 are shown in Figure 5. At most stations, ^{137}Cs showed higher concentrations in the surface sediment and decreased with increasing sediment detpth. In the coastal region (≤100m), significant proportion of accident-derived ^{137}Cs migrated to deeper sediment layers. In these coastal stations, typical structures of vertical mixing were observed from $^{210}Pbx_{ex}$ profiles (data are shown in Appendix A3), and considerable population of macrobenthos, such as polychaetes (*Capitellidae gen sp*., *Maldanella sp.*), were observed in the 3-15 cm sedimentary layers. In the vicinity of the FDNPP (St. NP0 and NP1), unusually high concentrations of ^{137}Cs, exceeding 1,000 Bq kg^{-1}, were observed in a subsurface horizon in each core. Although the general distribution of the accident-derived radiocesium in sediment was established by deposition of dissolved radiocesium in the early stage after the accident, a scattering of debris particles during the explosion of the FDNPP's facility in March 2011 has also pointed out as a mechanism bringing radiocesium to the seabed in the vicinity of the FDNPP (Adachi et al., 2013). Such a heterogeneous distribution of ^{137}Cs in the seabed sediment would be derived by a local deposition of highly ^{137}Cs-enriched particles.

On the contrary to the coastal region, most (>94%) ^{137}Cs in the offshore sediment remained in the upper 10 cm. The ^{137}Cs concentrations showed a maximum in the intermediate (2-5 cm) layer in several offshore stations (St. K6 and J7, Fig. 5).

4. Discussion

4.1 Resuspension as a potential process affecting radiocesium inventory in surface sediment

The ^{137}Cs concentrations in the coastal sediment generally decreased within a certain range variation (Fig. 4b), regardless of the wide range of initial inventory (concentration) of ^{137}Cs (Fig. 4c). It can be considered that a common mechanism might have affected the decrease of ^{137}Cs concentrations in the coastal sediments. In the following subsections, the relative importance of the three major

mechanisms that seem to be particularly important for the decrease of the sedimentary ^{137}Cs concentration, is discussed. Since the primary purpose of this paper is to overview the general temporal change occurring in a mesoscale (10-100km) area, discussion of local and "expectable" processes are only minimally presented.

Firstly, we focus on the loss of sedimentary radiocesium due to lateral transport of surface sediment. Fine sediment particles generally have higher concentrations of radionuclides due to their larger specific surface area (e.g., Abril and Fraga, 1996), and this tendency was observed in the seabed sediments after the FDNNP accident (Otosaka and Kobayashi, 2013; Ambe et al., 2014). It has also been suggested that such high concentrations of ^{137}Cs are also influenced by a high content of organic matter in the sediment (Ono et al., 2015). Recent field observations in the coastal area off Fukushima pointed out that westward long period waves often increase the shear stress near the seabed, and induce resuspension of bottom sediment (Yagi et al., 2015). This effect is temporally enhanced by stormy weather, and turbidity near the seafloor during storms approaches 10 ppm. Although it is difficult to generalize on the relationship between the waves and mobility of suspended particles, it is reasonable that highly mobile (i.e., small and low density) particles on the coastal seafloor can be resuspended during storms and exported laterally. Nevertheless, assuming that the turbidity is 10 ppm and the thickness of the highly turbid water is 50 m, the mass of suspended particles would be 0.5 kg m^{-2}, equivalent to only 0.3% of sediment in the 0-10 cm layer (~150 kg m^{-2}). If such storms take place 20 times a year, the loss of seabed sediment is estimated to be only about 6%, and is insufficient to reduce 30% of ^{137}Cs inventory in the surface sediment.

In the coastal region in this study area, it is reported that ^{137}Cs concentrations in highly-mobile fine particles (<75 μm) have several times (~ 6 times) higher than those in coarse sand (Otosaka and Kobayashi, 2013). However, the abundance of ^{137}Cs associate with fine particles in August 2011 was only 24% of the total ^{137}Cs in the sediment (Otosaka and Kobayashi, 2013). Therefore, the export of the fine particles hardly decreases the inventory of ^{137}Cs in sediment continuously at a rate of 30% year^{-1}.

As another estimation, the potential of lateral transport of the suspended particulate radiocesium between the coastal and offshore regions is assessed. In

the coastal region, from the results in Table 3, it can be estimated that about 0.13 PBq of ^{137}Cs have potentially been "exported" to the offshore or outside of this study area between 2011 and 2015. Time-series sediment traps deployed at 800 m depth at approximately 100 km southwest of FDNNP actually observed the export of "coastal" particulate radiocesium to the offshore seabed (Buesseler et al., 2015). However, Table 3 also indicates that the increased amount of sedimentary ^{137}Cs in the offshore region until the end of 2015 (+0.01PBq) corresponds to only 6% of the initial ^{137}Cs inventory in the coastal sediment (0.16 PBq). Assuming that the increase of sedimentary ^{137}Cs in the offshore region is caused by lateral transport of ^{137}Cs-bound particles from the coast, the annual export rate of particulate ^{137}Cs from the coastal area to the offshore in the 4.8 years is calculated to be about 1.3% year^{-1}. This value generally corresponds with the results from the sediment trap experiments (Buesseler et al., 2015), estimating that only 1-2% of sedimentary radiocesium is transported laterally to the offshore annually. These estimates also support the conclusion that the transport of suspended particles between coastal and offshore sediments is insufficient to significantly reduce ^{137}Cs inventories in the coastal sediments.

4.2 Effect of leaching of sediment-bound radiocesium

Many studies have suggested that radiocesium is almost irreversibly adsorbed on the surface of clay minerals (e.g., Comans et al., 1991). This irreversibility has also been supported by suspension experiments using seabed sediments (Otosaka and Kobayashi, 2013) and suspended particles (Takata et al., 2015) collected from in the surrounding regions off Fukushima, indicating that the dissolvable ^{137}Cs fractions are less than 10% of total particulate ^{137}Cs. However, these experiments were carried out under a closed system (^{137}Cs is in equilibrium), and might therefore underestimate the effect of desorption of ^{137}Cs from the particles. Recent field measurements off Fukushima have observed that dissolved ^{137}Cs concentrations in the seawater, overlying the seabed, are several times higher than levels in the intermediate layers of the water column (Otosaka et al., in prep.). This indicates that the leaching of ^{137}Cs from sediments should not be ignored from a long-term viewpoint.

Unfortunately, there is only limited data to quantify the benthic flux of the desorption of ^{137}Cs from the seabed, but assuming that the residence time of pore water is long (weeks or longer), and ^{137}Cs is in an equilibrium between the pore water and sediment with a typical distribution coefficient (K_d: 3,500 L kg^{-1}; IAEA, 2004), benthic flux of ^{137}Cs from the sediment (F_{CS}) can be estimated using Fick's Law (eqs. 6 and 7),

$$F_{cs} = D_{cs} \times \varphi \times \left(\frac{Cpw - Cbw}{\Delta Z}\right) \qquad (6)$$

$$C_{pw} = C_{sed} / K_d \qquad (7)$$

where, D_{CS}, φ, and ΔZ are whole sediment diffusion coefficient of Cs, porosity of the sediment, and thickness of the diffusion boundary layer, respectively. C_{pw}, C_{bw}, and C_{sed} are concentrations of ^{137}Cs in pore water, overlying water, and sediment, respectively.

Assuming D_{CS} = 2.2×10^{-5} m^2 day^{-1} (Li and Gregory, 1974), φ = 0.41 (typical value in this study), C_{bw} = 0 Bq L^{-1}, and ΔZ = 1×10^{-4} m (Santschi et al., 1983), as a high estimate, F_{CS} is expressed as 0.026×C_{sed} Bq m^{-2} day^{-1}. As the typical dry bulk density of sediment was 1.3 g mL^{-1} (Appendix A2), Cs inventory in the surface sediment (with 10 cm thickness) is calculated to be 130×C_{sed} Bq m^{-2}. Accordingly, the diffusion of ^{137}Cs from the sediment to the overlying water can reduce 0.02% of ^{137}Cs inventory in sediment in a day, and it indicates that about 7% of ^{137}Cs can be desorbed from the surface sediment in a year. This estimate suggests that the leaching of ^{137}Cs from the sediment cannot reduce the measured decrease of ^{137}Cs inventory of 27% year^{-1} in the surface sediment, while the ^{137}Cs benthic flux definitely increases concentrations in the overlying water. Additionally, assuming that the porosity of sediment is 0.41 and K_d is 3,500 kg L^{-1}, the ^{137}Cs abundance in the pore water is less than 0.01% of the ^{137}Cs inventory in the surface sediment. Even if the pore water is completely exchanged with the less-contaminated overlying water several times in a year, the loss of sedimentary ^{137}Cs by the exchange of pore water would be negligible.

4.3 Effect of vertical mixing of sediment

In Figure 6, biodiffusion coefficients (D_b) estimated from the vertical gradient of $^{210}Pb_{ex}$ are plotted against bottom depth. The D_b data were obtained from eight stations where the water depth ranges from 75 m to 1175 m. Estimated D_bs ranged between 0.06 and 21 cm^2 year^{-1}, and generally decreased with increasing depth. This tendency agrees with estimates reported by previous studies (hatched areas in Fig. 6). The D_bs of this study also agrees with the value estimated inversely from typical vertical distribution of sedimentary ^{137}Cs in the semi-offshore (100-200 m) region of Fukushima (Ambe et al., 2014).

Since a significant vertical gradient of $^{210}Pb_{ex}$ was not found in the coastal region (≤100 m depth) due to the rapid apparent sedimentation rate as well as low input of ^{226}Ra-supported ^{210}Pb, no $^{210}Pb_{ex}$-based D_bs are plotted in Figure 6 for the coastal region. Nevertheless, we can consider that the D_b in the coastal region is not less than10 cm^2 year^{-1}.

This D_b, of 10 cm^2 year^{-1}, is only a minimum value to be applied to the coastal region, and the actual D_b values in the region would be higher. In order to estimate a "realistic" D_b in the coastal region, the D_bs were inversely estimated from the temporal change of ^{137}Cs inventory in the surface sediment. In Figure 7, four examples of simulated temporal change of ^{137}Cs inventory are illustrated. The decreasing rate estimated with a minimum D_b (10 cm^2 year^{-1}) was about 10% year^{-1}, and was insufficient to reproduce the actual rate (-27% year^{-1}). On the other hand, the decrease was reproduced with a higher D_b, 200 cm^2 year^{-1}. Interestingly, the simulated temporal change in the ^{137}Cs inventory does not show a constant rate of decrease, and it seems to represent an actual trend (e.g. Fig. 2b).

The "realistic" D_b, 200 cm^2 year^{-1}, is 1-3 orders of magnitude higher than values in offshore regions, and 5 orders of magnitude lower than that at a beach (> 10^7 cm^2 year^{-1}: Nadaoka et al., 1981)(Fig. 6). Considering that the wave base regularly approaches the seabed in the shallow regions less than 20 m depth (e.g., Sawaragi, 1995), the D_b in these regions might exceed 200 cm^2 year^{-1}. On the other hand, typical D_bs in the temperate zone fall within the range of 10-200 cm^2 year^{-1} (Teal et al., 2008). For a conservative estimate, we conclude that the possible D_b values in the coastal (≤100 m) region range between 10 and 200 cm^2 year^{-1}.

In Figure 5, observed and simulated distributions of ^{137}Cs are shown for comparison. Lines in Figure 5 indicate simulated profiles of the ^{137}Cs concentration. In the stations, deeper than 75 m depth, simulated profiles are based on the $^{210}Pb_{ex}$ based D_b value at the corresponding station. For the two stations less than 75 m depth (St. NP0 and NP1), D_b was provisionally given as 200 cm^2 $year^{-1}$.

In the hemipelagic stations (>900 m), modeled ^{137}Cs profiles in the sediment agreed well with the observed ones. This result indicates that the vertical profiles of sedimentary ^{137}Cs in this region were dominated by vertical mixing. Although it is reported that resuspension of the surface sediment takes place in the hemipelagic region (e.g., Otosaka et al., 2014), the extent is quite limited and such turbulence barely changes the vertical structures of the sediment. Therefore, the vertical mixing in the hemipelagic stations would be dominated by bioturbation.

In the semi-offshore stations (water depth: 75-300 m), except for Sta. J11, observed vertical profiles of ^{137}Cs generally agreed with the simulated data, but relatively lower in the upper (~5 cm) layers. Such a deficit of ^{137}Cs in the upper layer of sediment would be attributed to the effect of resuspension and desorption of sedimentary ^{137}Cs, as described in the previous subsections. These results also suggest that the vertical profiles of ^{137}Cs in sediment were mainly controlled by the vertical mixing of sediment, and the other processes affected only the upper part of sedimentary layers.

Among the semi-offshore stations, only J11 did not show the deficit of ^{137}Cs in the surface sediment. This exceptional station is located on the outer edge of Sendai Bay, adjacent to where the Abukuma River enters to the ocean. The Abukuma River is the largest river flowing into the study area, and supplies one third of the total river discharge of particulate radiocesium (Yamaguchi et al., 2014). As far as we can see from Figure 4, the variation rate for sedimentary ^{137}Cs concentration in Sendai Bay (38.2°N - 38.3°N) is around -30 % $year^{-1}$ and can be considered as a “typical” rate. This indicates that terrestrial-particles-bound ^{137}Cs is not accumulated in Sendai Bay. Detailed observations in Sendai Bay by Kakehi et al. (2016) also reported that there is no notable local accumulation of riverine particles in the bay except within brackish estuaries. Accordingly, the remarkable accumulation of ^{137}Cs in the upper part of the sediment at Sta. J11, is thought to

be caused by lateral transport of terrestrial particle-bound ^{137}Cs to the outer edge of Sendai Bay.

At the nearshore stations (NP0 and NP1), shallower than 54 m depth, significant vertical change of ^{137}Cs concentration was not observed, and except for the horizons with anomalously high ^{137}Cs concentration, the observed profiles agreed with simulated ones based on a maximum D_b value (200 cm^2 year^{-1})(Fig. 5). Similarly to the semi-offshore stations, observed ^{137}Cs concentrations in the upper layers were lower than those of the simulated ones. From these results, we conclude that the accident-derived ^{137}Cs migrated to the lower layers of the sediment via vertical mixing, and the extent is greater in shallower regions.

4.4 Budget of ^{137}Cs in the surface sediment

Processes affecting the variation of ^{137}Cs concentrations in the surface sediments are summarized in Figure 8. Assuming that the coastal sediment had been mixing with a minimum biodiffusion coefficient, D_b, of 10 cm^2 year^{-1}, it is estimated that about 43% of sedimentary radiocesium migrated to the deeper sedimentary layers (i.e., below 10 cm) between March 2011 and December 2015 (4.8 years). As shown in Table 3, the variation rate (X) of ^{137}Cs inventory in nearshore sediment is -27% year^{-1} (the exponent α is -0.32 year^{-1} from eq. (2)), and the result indicates that about 22% of ^{137}Cs remained in the surface (top 10 cm) sediment. Accordingly, it can be inferred that more than 65% of the initially deposited ^{137}Cs has remained in the nearshore sediment. Furthermore, if the D_b is set as 200 cm^2 year^{-1}, the decrease in ^{137}Cs inventory in the surface sediment can be explained by the transport to the deeper layers. Considering that about 22% of the initial ^{137}Cs has remained in the top 10 cm sediment and about 6 % of initial deposition of ^{137}Cs to sediment is considered to be transported to the offshore sediment (Table 3), it can be estimated that 72% of ^{137}Cs has been transported to the deeper layers. These estimates indicate that the majority of ^{137}Cs deposited to the coastal region has remained in the sediment.

On the other hand, this estimation also indicates that at most 29% of sedimentary ^{137}Cs might have dissolved or been dispersed associated with fine particles within the 4.8 years. Assuming a constant rate of the loss of ^{137}Cs from the sediment, the annual elimination rate is estimated to be 7%, and this rate

approximately agrees with the loss of ^{137}Cs-bound particles (1.3% year^{-1}; subsection 4.1) and dissolution of ^{137}Cs (7% year^{-1}; subsection 4.2) from coastal sediment. Therefore, it can be concluded that the mass balance of ^{137}Cs illustrated in Figure 8 represents the general movement of sedimentary ^{137}Cs within the 4.8 years.

5. Conclusion

In this paper, temporal change in the concentration of ^{137}Cs in the surface sediment (0-10 cm) between 2011 and 2015 observed in a 150 km radius of FDNPP is outlined, and the primary factors affecting the temporal change was inferred.

In the coastal region, about 80% of the initially-deposited ^{137}Cs in the surface sediment had dissipated by the end of 2015. As the abundance of radionuclides in the surface sediment affects the radioactive levels in benthic organisms, possible ^{137}Cs dose effects on the benthic ecosystem might have decreased with time.

In the meantime, it was estimated that the primary process affecting the decrease of ^{137}Cs concentrations in the coastal surface sediment was the vertical mixing of sediments. This indicates that the majority of the ^{137}Cs in the coastal sediment has not been exported to other regions, but migrated to the deeper sedimentary layers (>10 cm). Although the export of particle-bound ^{137}Cs and dissolution of ^{137}Cs from the coastal sediment is also crucial to reduce the ^{137}Cs inventory, the contribution is considered to be minor.

Needless to say, further understanding of the local-scale behavior of ^{137}Cs-bound particles, such as flushing of the particles during storm weather, is essential to better predict the fate of the accident-derived radionuclides near the seabed. The larger-scale mass balance of sedimentary ^{137}Cs suggested by this study would be a benchmark for the integration of local-scale behaviors of particulate ^{137}Cs from a long-term viewpoint.

Acknowledgements

The author is grateful to captains, crews and scientists of the R/V Tansei-Maru KT-11-27, KT-13-01, R/V Hakuho-Maru KH-11-07, R/V Shinsei-Maru KS-14-20, KS-15-13 (Univ of

Tokyo/JAMSTEC), and R/V Seikai (JAEA) cruises for their assistance in the fieldwork. The author is also grateful to J. Nishikawa, H. Narita, Y. Kato (Tokai Univ.), T. Aono, M. Fukuda (QST), M. Uematsu, H. Obata (Univ. Tokyo), H. Tazoe (Hirosaki Univ.), M.C. Honda (JAMSTEC), K.O. Buesseler (WHOI), S. Nagao (Kanazawa Univ.), T. Morita, T. Ono, H. Kaeriyama, D. Ambe (Natl. Res. Inst. Fish Sci., Japan), T. Kobayashi, H. Kawamura, T. Nakanishi, E. Takeuchi, M. Watanabe, Y. Kumagai, Y. Segawa, Y. Satoh, M. Nakano, T. Isozaki, M. Nemoto, K. Tobita, M. Nagaoka, M. Hirasawa, K. Matsumura (JAEA) for their support in the field, laboratory work and their valuable comments. The manuscript was improved by two helpful reviews.

References

Abril JM, Fraga E (1996) Some physical and chemical features of the variability of k_d distribution coefficients for radionuclides. J Environ Radioact 30: 253-270

Adachi K, Kajino M, Zaizen Y, Igarashi Y (2013) Emission of spherical cesium-bearing particles from an early stage of the Fukushima nuclear accident. Sci Rep 3:2554. doi:10.1038/srep02554.

Ambe D, Kaeriyama H, Shigenobu Y, Fujimoto K, Ono T, Sawada H, Saito H, Miki S, Setou T, Morita T, Watanabe T (2014) Five-minute resolved spatial distribution of radiocesium in sea sediment derived from the Fukushima Dai-ichi Nuclear Power Plant. J Environ Radiact 138: 264-275

Black EE, Buesseler KO (2014) Spatial variability and the fate of cesium in coastal sediments near Fukushima, Japan. Biogeosci 11: 5123-5137

Buesseler KO, German CR, Honda MC, Otosaka S, Black EE, Kawakami H, Manganini SJ, Pike SM (2015) Tracking the fate of particle associated Fukushima Daiichi cesium in the ocean off Japan. Environ Sci Technol 49: 9807-9816

Buesseler KO, Dai M, Aoyama M, Benitez-Nelson, Charmasson S, Higley K, Medrich V, Masque P, Oughton D, Smith JN (2017) Fukushima Daiichi–derived radionuclides in the ocean: Transport, fate, and impacts. Annu Rev Mar Sci 9: 173-203

Cochran JK (1985) Particle mixing rates in sediments of the eastern equatorial Pacific: Evidence from ^{210}Pb, ^{239,240}Pu and ^{137}Cs distributions at MANOP sites. Geochim Cosmochim Acta 49: 1195-1210

Comans RN, Haller M, De Preter P (1991) Sorption of cesium on illite: Non-equilibrium behaviour and reversibility. Geochim Cosmochim Acta 55: 433-440

Fukuda M, Aono T, Yamazaki S, Nishikawa J, Otosaka S, Ishimaru T, Kanda J (2016) Dissolved radiocaesium in seawater off the coast of Fukushima during 2013-2015. J Radioanal Chem: doi:10.1007/s10967-016-5009-9

IAEA (2003) Collection and Preparation of Bottom Sediment Samples for Analysis of Radionuclides and Trace Elements. IAEA TECDOC 1360, International Atomic Energy Agency, Vienna, pp. 130

IAEA (2004) Sediment Distribution Coefficients and Concentration Factors for Biota in the Marine Environment. IAEA Technical Report Series 422, International Atomic Energy Agency, Vienna, pp. 95

Ikehara K, Irino T, Usami K, Jenkins R, Omura A, Ashi J (2014) Possible submarine tsunami deposits on the outer shelf of Sendai Bay, Japan resulting from the 2011 earthquake and tsunami off the Pacific coast of Tohoku. Mar Geol 349: 91-98

Iwata K, Tagami K, Uchida S (2013) Ecological half-lives of radiocesium in 16 species in marine biota after the TEPCO's Fukushima Daiichi Nuclear Power Plant accident. Environ Sci Technol 47: 7696-7703

Kanda J (2013) Continuing ^{137}Cs release to the sea from the Fukushima Dai-ichi Nuclear Power Plant through 2012. Biogeosci 10: 6107-6113

Kakehi S, Kaeriyama H, Ambe D, Ono T, Ito S, Shimizu Y, Watanabe T (2016) Radioactive cesium dynamics derived from hydrographic observations in the Abukuma River Estuary, Japan. J Environ Radioact 153: 1-9

Li YH, Gregory S (1974) Diffusion of ions in sea-water and in deep-sea sediments. Geochim Cosmochim Acta 38: 703-714

MAFF (Ministry of Agriculture, Forestry and Fisheries), Japan (2016) Results of the monitoring on radioactivity level in fisheries products. http://www.jfa.maff.go.jp/e/inspection/index.html. Accessed 13 March 2017

MOE (Ministry of the Environment), Japan (2013) Results of the monitoring survey after the Great East Japan earthquake (in Japanese). http://www.env.go.jp/jishin/monitoring/results_me.html. Accessed 13 March 2017

MOE (2016a) Results of the 2014 monitoring survey after the Great East Japan earthquake (in Japanese). http://www.env.go.jp/press/files/jp/102775.pdf. Accessed 13 March 2017

MOE (2016b) Results of the 2015 monitoring survey after the Great East Japan earthquake (in Japanese). http://www.env.go.jp/jishin/jishin/waste/101662/bessi_4.pdf. Accessed 20 January 2017

Misumi K, Tsumune D, Tsubono T, Tateda Y, Aoyama M, Kobayashi T, Hirose K (2014) Factors controlling the spatiotemporal variation of ^{137}Cs in seabed sediment off the Fukushima coast: implications from numerical simulations. J Environ Radioact 136: 218-228

Murota K, Saito T, Tanaka S (2016) Desorption kinetics of cesium from Fukushima soils. J Environ Radioact 153: 134-140

Nadaoka K, Tanaka N, Katoh K (1981) Field observation of local sand movements in the surf zone using fluorescent sand tracer. Port Harbour Res Inst Rep, 20: 75-126

NOAA (National Oceanic and Atmospheric Administration), US (2006) 1-Minute Gridded Global Relief Data (ETOPO2v2), NOAA National Geophysical Data Center, Boulder

NRA (Nuclear Regulation Authority), Japan (2016) Monitoring information of environmental radioactivity level. http://radioactivity.nsr.go.jp/en/list/205/list-1.html. Accessed 13 March 2017

Oikawa S, Takata H, Watabe T, Misonoo J, Kusakabe M (2013) Distribution of the Fukushima-derived radionuclides in seawater in the Pacific off the coast of Miyagi, Fukushima, and Ibaraki Prefectures, Japan. Biogeosci 10: 5031-5047

Okamura H, Ikeda S, Morita T, Eguchi S (2016) Risk assessment of radioisotope contamination for aquatic living resources in and around Japan. Proc Natl Acad Sci USA 113: 3838-3843

Ono T, Ambe D, Kaeriyama H, Shigenobu Y, Fujimoto K, Sogame K, Nishiura N, Fujikawa T, Morita T, Watanabe T (2015) Risk assessment of radioisotope contamination for aquatic living resources in and around Japan. Geochem J 49: 219-227

Otosaka S, Kobayashi T (2013) Sedimentation and remobilization of radiocesium in the coastal area of Ibaraki, 70 km south of the Fukushima Dai-ichi Nuclear Power Plant. Environ Monit Assess 185: 5419-5433

Otosaka S, Kato Y (2014) Radiocesium derived from the Fukushima Daiichi Nuclear Power Plant accident in seabed sediments: initial deposition and inventories. Environ Sci: Processes Impacts 16: 978-990. doi:10.1039/c4em00016a

Otosaka S, Nakanishi T, Suzuki T, Satoh Y, Narita H (2014) Vertical and lateral transport of particulate radiocesium off Fukushima. Environ Sci Technol 48: 12595-12602

Saito K, Tanihata I, Fujiwara M, Saito T, Shimoura S, Otsuka T, Onda Y, Hoshi M, Ikeuchi Y, Takahashi F, Kinouchi N, Saegusa J, Seki A, Takemiya H, Shibata T (2015) Detailed deposition density maps constructed by large-scale soil sampling for gamma-ray emitting radioactive nuclides from the Fukushima Dai-ichi Nuclear Power Plant accident. J Environ Radioact 139: 308-319

Santschi PH, Bower P, Nyffeler UP, Azevedo A, Broecker WS (1983) Estimates of the resistance to chemical transport posed by the deep-sea boundary layer. Limnol Oceanogr 28: 899-912.

Sawaragi T (1995) Coastal Engineering - Waves, Beaches, Wave-Structure Interactions, Elsevier, Amsterdam, pp. 478

Seike K, Kitahashi T, Noguchi T (2016) Sedimentary features of Onagawa Bay, northeastern Japan after the 2011 off the Pacific coast of Tohoku Earthquake: sediment mixing by recolonized benthic animals decreases the preservation potential of tsunami deposits. J Oceanogr, 72: 141-149.

Takata H, Hasegawa K, Oikawa S, Kudo N, Ikenoue T, Isono RS, Kusakabe M (2015) Remobilization of radiocesium on riverine particles in seawater: The contribution of desorption to the export flux to the marine environment. Mar Chem 176: 51-63

Tateda Y, Tsumune D, Tsubono T (2013) Simulation of radioactive cesium transfer in the southern Fukushima coastal biota using a dynamic food chain transfer model. J Environ Radioact 124: 1-12

Tateda Y, Tsumune D, Misumi K, Aono T, Kanda J, Ishimaru T (2017) Biokinetics of radiocesium depuration in marine fish inhabiting the vicinity of the Fukushima Dai-ichi Nuclear Power Plant. J Environ Radioact 166: 67-73

Teal LR, Bulling MT, Parker ER, Solan M (2008) Global patterns of bioturbation intensity and mixed depth of marine soft sediments. Aquat Biol 2: 207-218

TEPCO (Tokyo Electric Power Co.) (2016) Analysis results of radioactive materials obtained at each sampling location. http://www.tepco.co.jp/en/nu/fukushima-np/f1/smp/index-e.html. Accessed 13 March 2017

Wang C, Baumann Z, Madigan DJ, Fisher NS (2016) Contaminated marine sediments as a source of cesium radioisotopes for benthic fauna near Fukushima. Environ Sci Technol 50: 10448-10455

Yagi H, Sugimatsu K, Kawamata S, Nakayama A, Udagawa T (2015) Bottom turbidity, boundary layer dynamics, and associated transport of suspended particulate materials off the Fukushima coast. In: Nakata K, Sugisaki H (eds) Impacts of the Fukushima Nuclear Accident on Fish and Fishing Grounds, Springer, Tokyo, pp. 238

Yamaguchi M, Kitamura A, Oda Y, Onishi Y (2014) Predicting the long-term ^{137}Cs distribution in Fukushima after the Fukushima Dai-ichi nuclear power plant accident: a parameter sensitivity analysis. J Environ Radioact 135: 135-146

Figure legends

Figure 1. Sampling locations. Filled circles, open circles, and triangles indicate data from this study, Tokyo Electric Power Co., and Ministry of Environment, Japan, respectively.

Figure 2. Trend of ^{137}Cs concentrations in surface (0-10 cm) sediment collected from the coast of Miyagi (a: 38.97-37.90 °N), Fukushima (b: 38.97-37.90 °N), Ibaraki (c: 38.90-36.86 °N) Prefectures, and offshore (bottom depth >100m) regions. Activities were decay-corrected to March 11, 2011.

Figure 3. Plot of variation rate of sedimentary ^{137}Cs vs bottom depth. Distribution of median grain size (in Wentworth scale) is also shown at the top of the figure.

Figure 4. (a) Location of coastal (bottom depth <100m) stations, and latitudinal changes in (b) ^{137}Cs variation rate, (c) initial ^{137}Cs concentrations, and (d) variation index.

Figure 5. Vertical profiles of ^{137}Cs in sediment. Open circles and lines indicate observed and modelled profiles. Note changes in horizontal scales. Due to a lack of significant vertical change of $^{210}Pb_{ex}$ in stations NP0 and NP1, modelled ^{137}Cs profiles in those stations (dashed lines) were estimated using a representative biodiffusion coefficient in the coastal region (D_b = 200). In St. J11, S6, and J7, different Db values are used between the upper and deeper layers reflecting a difference of extent of disturbance.

Figure 6. Biodiffusion coefficient (D_b) vs bottom depth. Filled circles indicate data obtained by this study.

Figure 7. Temporal changes of ^{137}Cs concentrations in surface sediment modelled with different biodiffusion coefficient (D_b) values.

Figure 8. Schematic of mass balance of ^{137}Cs in the coastal seabed.

Table title

Table 1. Overview of the data sources

Table 2. Coefficient of variation between 2011 and 2015

Table 3. Variation rates and temporal changes in ^{137}Cs concentrations in surface sediment between 2011 and 2015

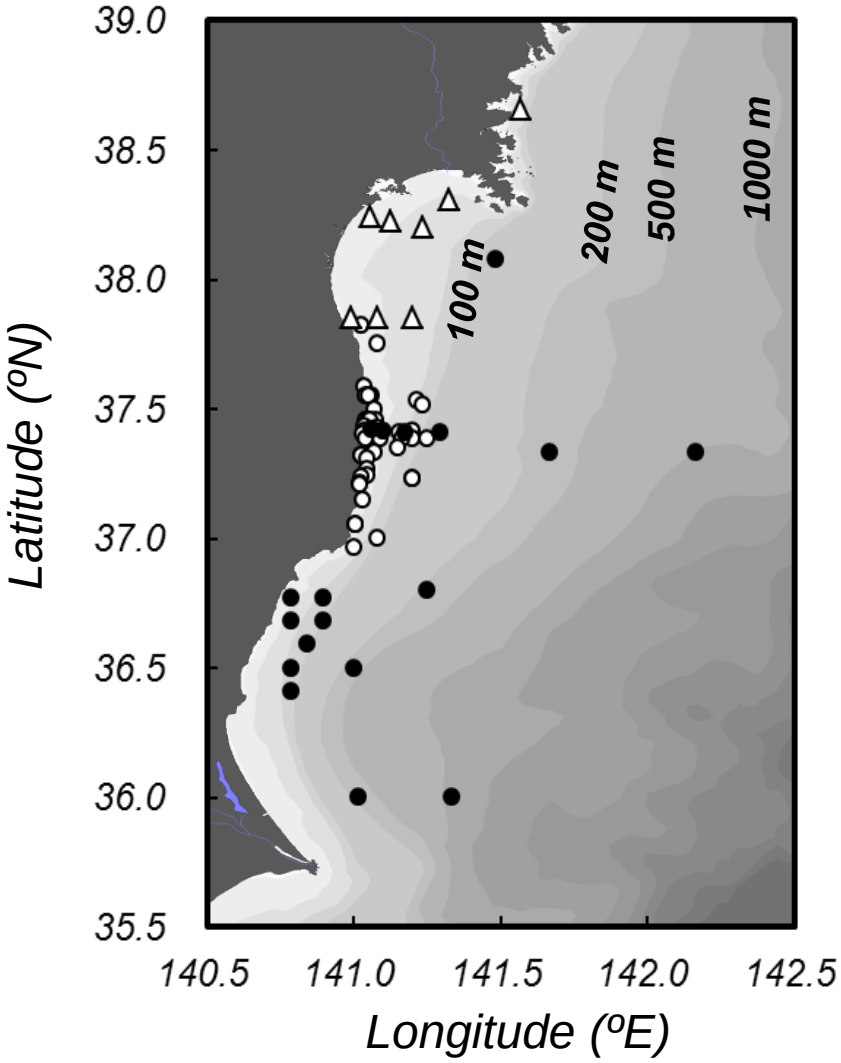

Otosaka, Fig. 1

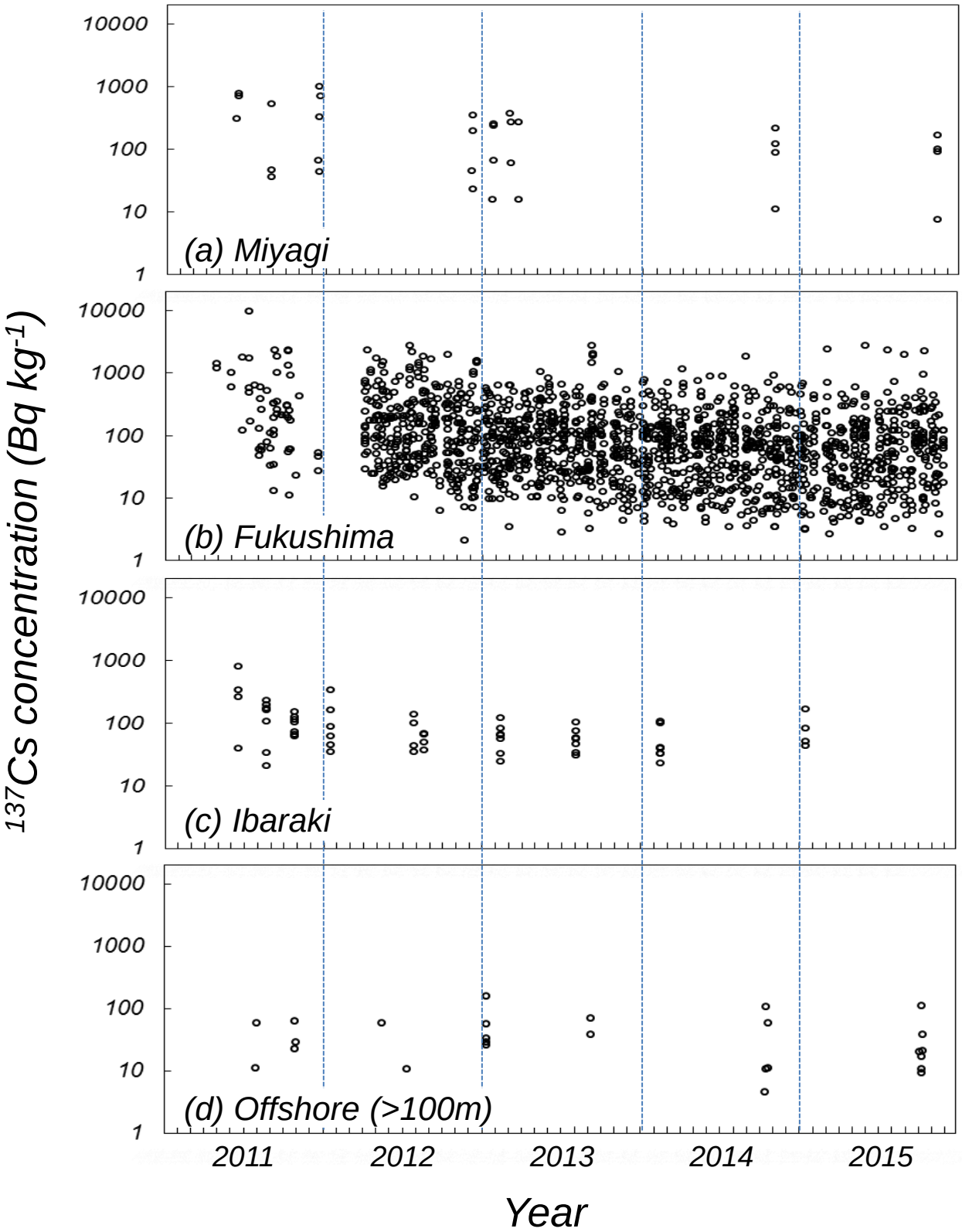

Otosaka, Fig. 2

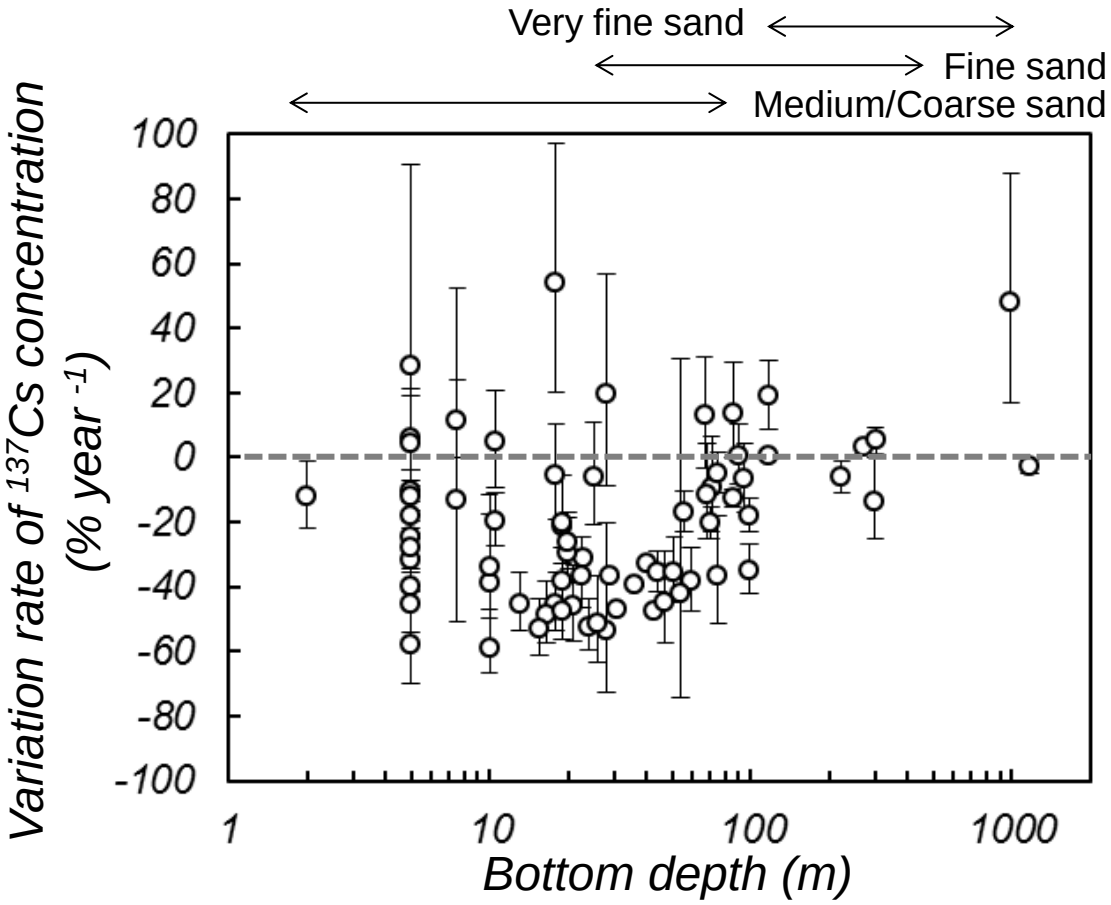

Otosaka, Fig. 3

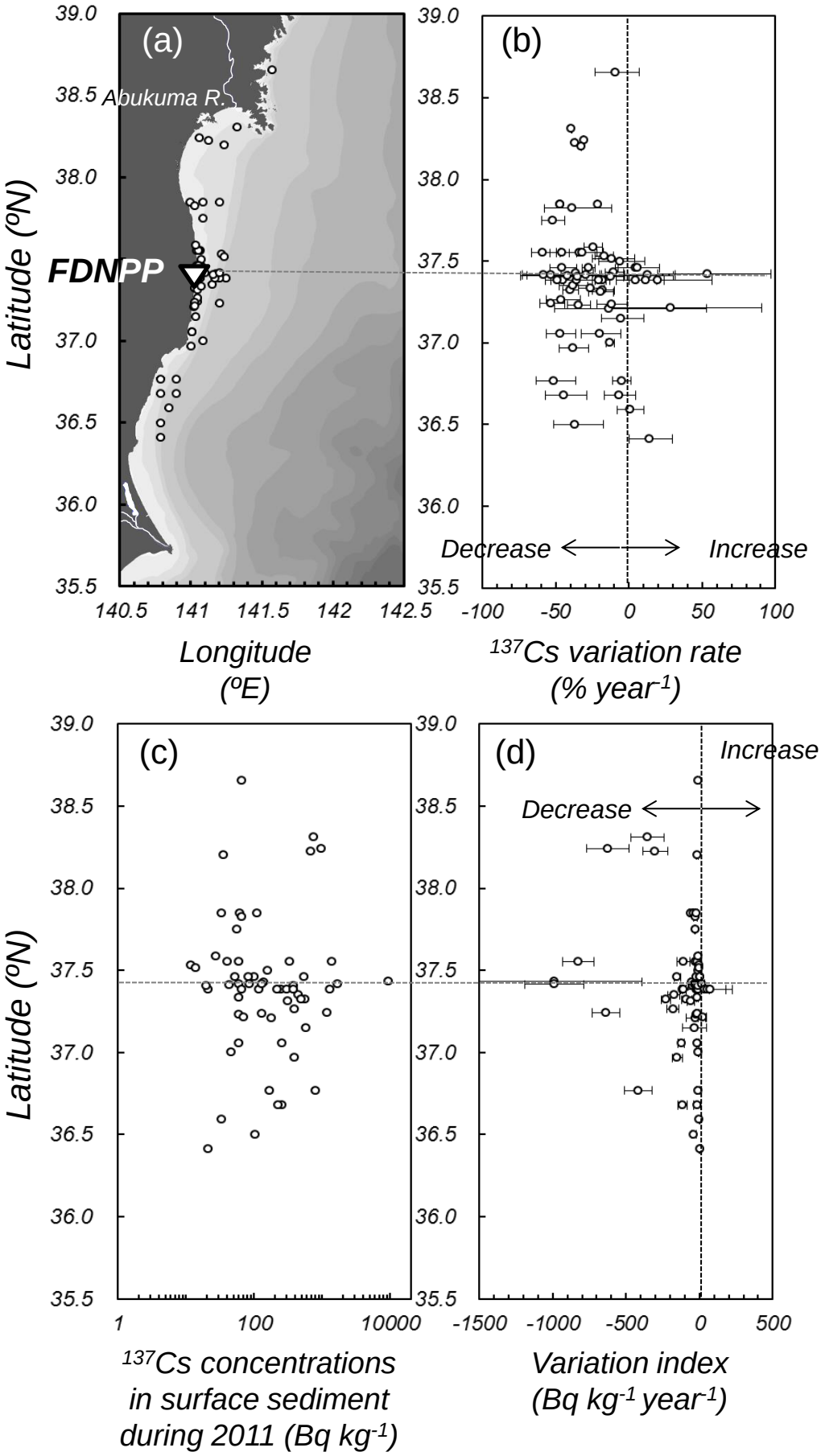

Otosaka, Fig. 4

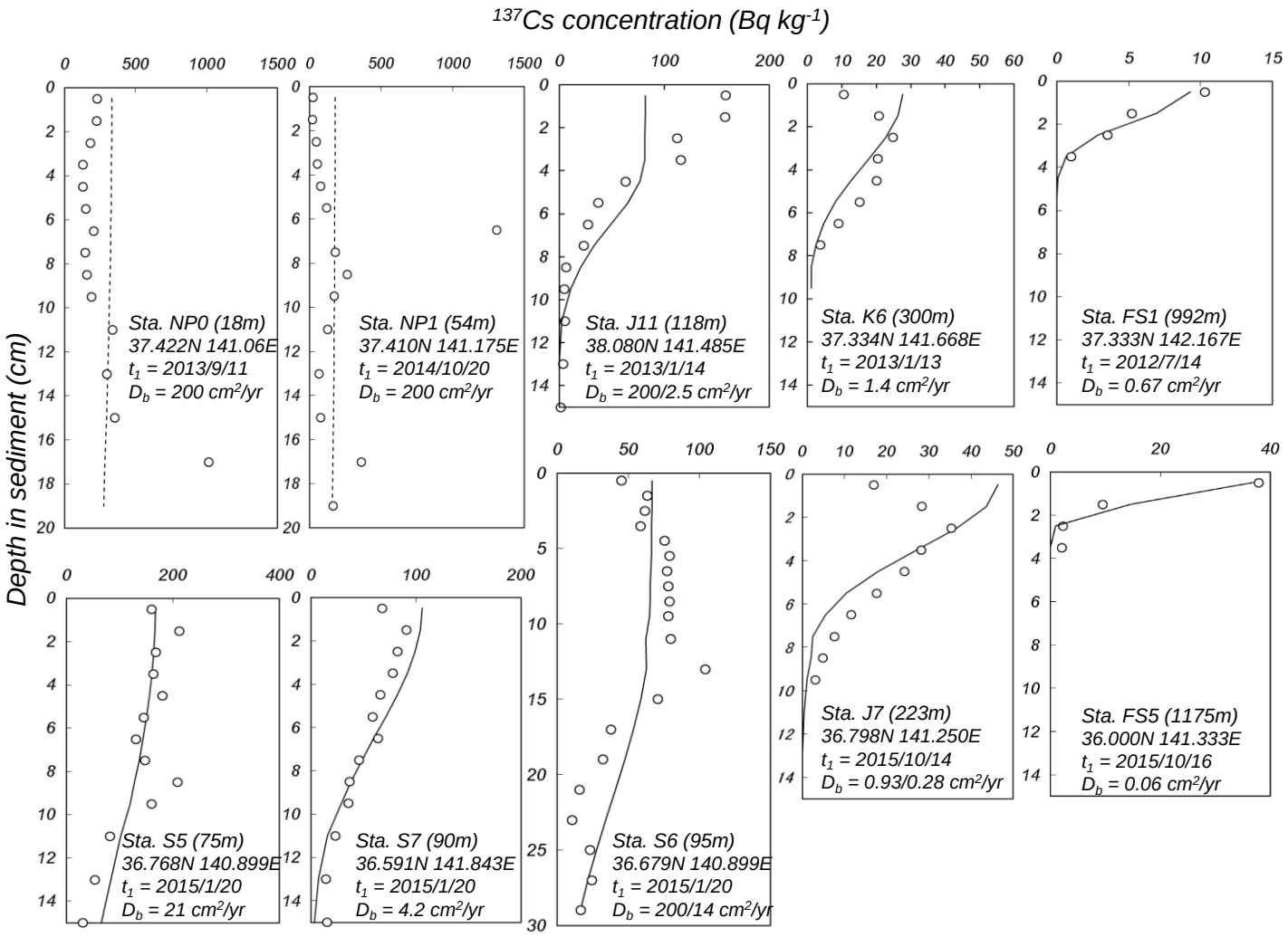

Otosaka, Fig. 5

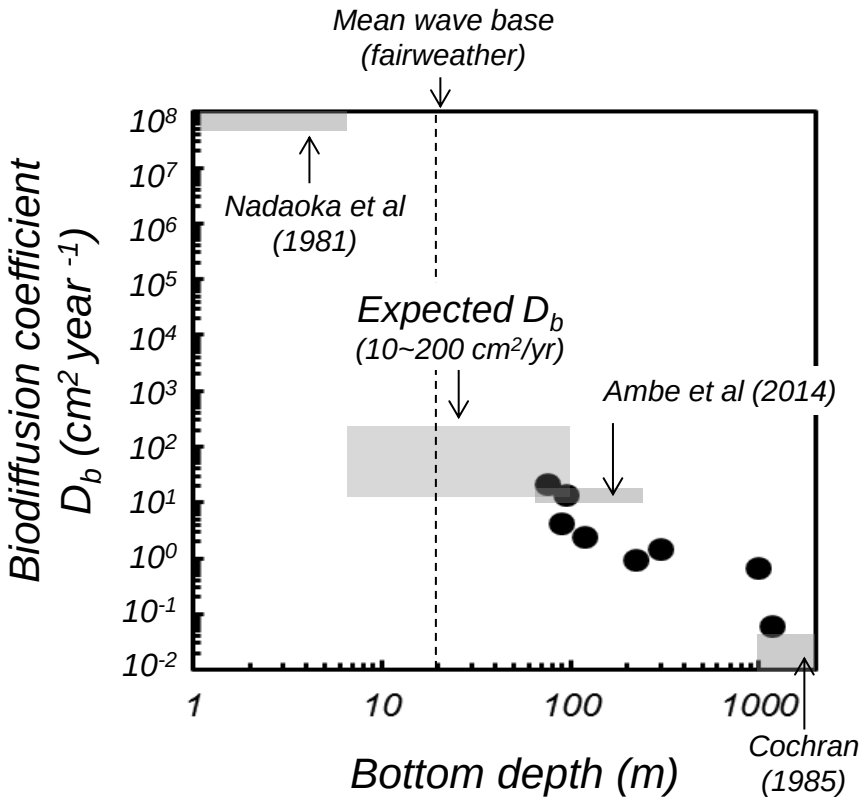

Otosaka, Fig. 6

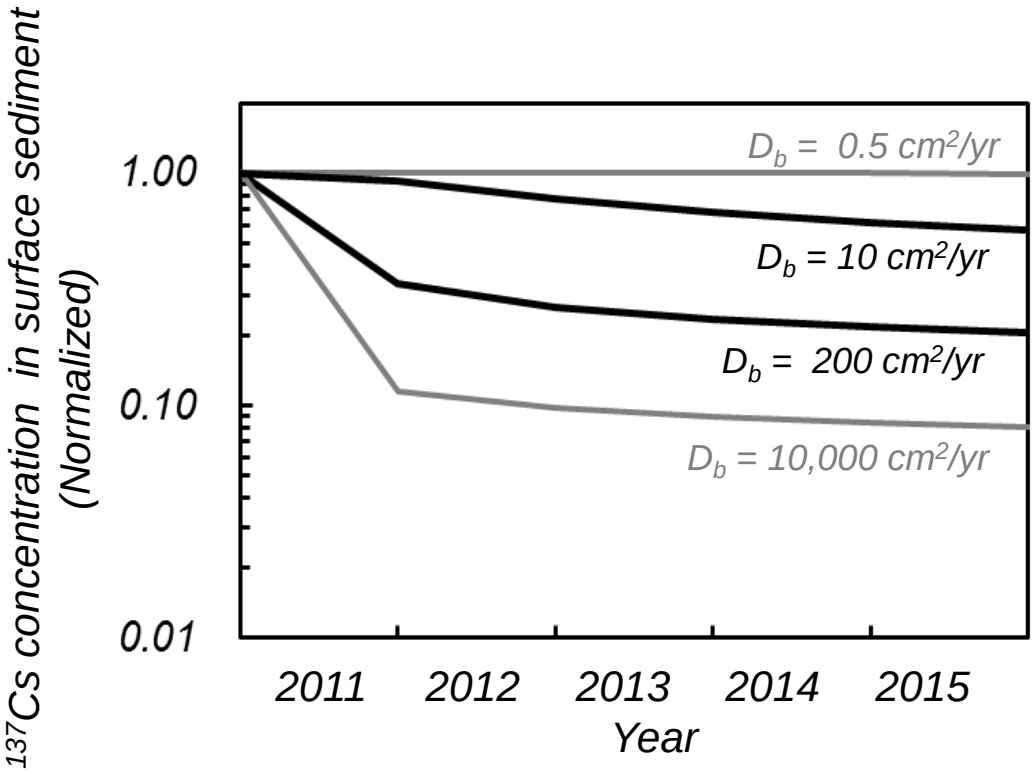

Otosaka, Fig. 7

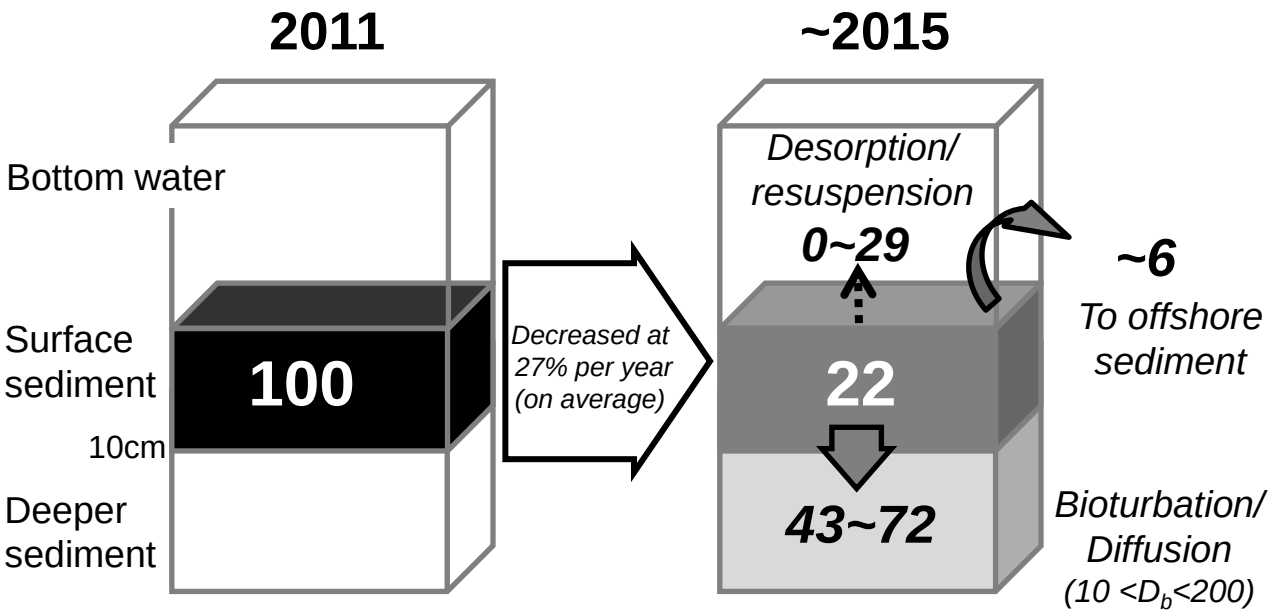

Otosaka, Fig. 8

Table 1 Overview of the data sources

Data source	Number of stations	Observation period	
		Start	End
This study	18	2011/6/20	2015/10/16
Ministry of Environment, Japan	8	2011/6/16	2015/11/21
Tokyo Electric Power Co., Japan	45	2011/4/29	2015/11/30

Table 2 Coefficient of variation between 2011 and 2015

Parameter	Number of stations	Coefficient of variation Median (Range)
Dry bulk density	18	6.7% (2.9−12.2%)
Median diameter	16	14.7% (1.0−36.1%)
Organic matter content	16	29.0% (7.2−74.7%)
^{137}Cs concentration (0-10 cm)	18	43.3% (1.1−124%)

Table 3 Variation rates and temporal changes in ^{137}Cs inventories in surface sediment

Area	Variation rate of ^{137}Cs inventory (% year^{-1})				Total ^{137}Cs inventory in 2011** (PBq)	Change in ^{137}Cs inventory between 2011 and 2015 (PBq)
	Mean*	Minimum	Maximum	n		
Nearshore (≤100m)	-27	-59	+54	63	0.16	-0.13
Offshore (>100m)	+5	-13	+48	8	0.036	+0.010

*Geometric mean
**Otosaka and Kato (2014)